On the Detection of Denrite Activity Using MRI

An Honors Thesis (HONRS 499)

by

William I. Jay

Thesis Advisor
Dr. Ranjith Wijesinghe

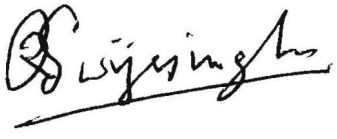

Ball State University
Muncie, Indiana

April 2012

Exected Date of Graduation
May 2012

Abstract

The currents associated with neural activity generate their own magnetic fields which potentially cause a measurable phase change in a magnetic resonance (MR) signal. The feasibility of directly measuring neural currents via magnetic resonance imaging (MRI) is still under debate. If direct imaging were possible, there would be immediate benefits for neurosurgeons, doctors studying degenerative diseases of the brain, neuroscientists, and others. In this thesis, individual dendrites are modelled as magnetic current dipoles on a variable lattice structure in order to calculate the magnetic fields and phase shifts generated by active neural tissue. The results show that the field produced by a dense collection of simultaneously active dendrites may be just detectable under the most ideal circumstances, but in almost every realistic case the field cannot be detected using current MRI technology.

Acknowledgements

The initial inspiration for this research stems from the work of Brian Dolasinki, a former student of Dr. Wijesinghe, who in his masters thesis addressed a similar question from a slightly different perspective. His thesis provided much guidance, particularly in reviewing the relevant literature. During the process of submitting a technical manuscript for publication in an academic journal, Dr. Bradley Roth of Oakland University (Rochester, MI) provided invaluable suggestions and corrections, many of which may now be found in this thesis.

Coming from a background in physics and mathematics, I have often found holes in my knowledge of biology and neuroscience, and I wish thank Dr. Kelly-Worden of the Department of Physiology and Health Science for helping me to fill in some of these gaps.

Since fall 2010 my research with Dr. Wijesinghe has been supported through a variety of sources. Although my research time has been split on a number of different projects, I gratefully acknowledge support along the way from the following sources:

- The Indiana Academy of Science
- An Honors Undergraduate Fellowship
- An ASPiRE travel grant
- The Department of Physics and Astronomy
- The College of Sciences and Humanities

Finally, Dr. Wijesinghe has been a constant support and wonderful mentor throughout the research process, and I offer my greatest thanks to him.

Contents

List of Figures

List of Tables

Chapter 1

Author Statement

In fall 2010 I began working as a research assistant under the supervision of Dr. Wijesinghe in Ball State's Medical Physics Laboratory. An eager junior just freshly returned from a year abroad, I had little idea what to expect at the time, but I realized the importance of beginning to work on some sort of research. Overall, this thesis represents the culmination of my research work as an undergraduate at Ball State University, and I would like to take this opportunity to call attention to some of the important lessons that I have learned along the way.

If asked to name a single skill that this research has developed, it would almost certainly be computer programming. Standing behind all the simulations presented in the second half of this thesis are several hundred if not a thousand or more lines of computer code in Matlab and Java. I make no claims regarding the elegance or clever efficiency of my programming, but for a student without an appreciable background in computer science, this work represents a significant achievement and one that might easily be overlooked in reading this thesis. Most importantly, I feel the research process has helped me to achieve a level of proficiency in programming that will allow me to attack real-world problems with computers in my life as a graduate student and professional scientist.

In addition to computer skills, the research experience has also developed my ability to learn independently, primarily through reading journal articles and textbooks. For someone trained in physics and mathematics, I found a steep learning curve in trying to decipher the technical language present (and necessary) in biomedical journals. I suspect this difficulty is common to entering any new academic field, and the experience will certainly be good preparation for graduate work, during which I plan to change directions and encounter an entirely different set of jargon.

On a more intangible level, I have enjoyed working on real-life research problems of current interest to scientists in the field. Although one may learn quite a bit from textbook problems, it is exciting to work on a problem that has never before been solved and whose solution is not necessarily certain to exist in the form one expects. Such are the problems that professional scientists typically

encounter, and my thesis research has helped strengthen my resolve to join their ranks.

Finally, it seems to me very important that scientists cultivate the ability to explain their (often abstract) work to the wider population, especially considering the government-funded nature of contemporary scientific research. In this spirit, I have endeavored to describe my research in a widely-accessible fashion, and trying my hand at this style of writing has been a thoroughly enjoyable process. My hope is that any student or faculty member within the Honors College could, given the interest, read and appreciate the main ideas of my work in what follows.

Chapter 2

General Introduction

As the title of this thesis suggests, my research straddles the usually disparate fields of physics and biology. Although this thesis approaches the problem primarily from a physical and mathematical perspective, a certain degree of familiarity with the relevant biological systems is necessary. Indeed, biology is the natural starting point for the discussion, since one must first orient oneself within the concrete, real-life system before beginning to describe it abstractly through the application of physical and mathematical models. For this reason, I begin with an introduction to neurobiology and the biology of the human brain in Chapter 3. Secondly, in order to understand the physical models, some knowledge of basic physics is necessary, and so I review the important concepts in Chapter 4. In Chapter 5, I introduce the basic underlying principles of magnetic resonance imaging (MRI), since they play a central role in everything that follows. My primary goal in providing these introductions is to make my thesis accessible to the widest possible audience. I recall my initial frustration at the beginning of my research as I tried to navigate the jungle of jargon characteristic of academic journals, and I hope that what follows may be largely self-contained. After these important introductions, the reader should be well-equipped to understand the arguments and methods presented in the final portion of this thesis.

Chapter 3

Neurobiology and the Biology of the Human Brain

As living organisms interact with the world around them, they receive a constant barrage of complex sensory information. The survival of these organisms depends critically on their ability to process and respond to this information. In humans and most other animals this is the job of the nervous system [28].

The fundamental functional units in the central nervous system are nerve cells, also called neurons. Neurons exchange information through chemical and electrical processes known together as neural signalling. A typical neuron (pictured below in Figure 3.1) is composed of several primary parts: the soma (or cell body), the axon, and a collection of dendrites. The soma contains the bulk of the neuron, including its nucleus, organelles, and cytoplasm and may range in size from 5 to 120 μm for a typical neuron [28]. The axon is the long, narrow extension of the cell responsible for the propagation of electrical signals between neurons; although axons typically have microscopic diameters on the order of tens of microns, they can extend for macroscopic distances up to a meter in length [40]. The other projections of the cell body are the short, finger-like dendrites [28]. Dendrites typically branch to form complex patterns, and these patterns provide a classification scheme for neurons (see Figure 3.2 below). Unipolar neurons are characterized by a spherical soma and single outgrowth which branches into two forks that contain the axon and dendrites. Bipolar neurons have an elongated soma with outgrowths containing the axon and dendrites on opposite ends. Multipolar neurons have an irregularly shaped soma; the axon extends away from the soma, while numerous dendrites branch directly off of the cell body. Multipolar neurons are the most numerous neurons in the human central nervous system, and among them another division exists. Golgi Type I multipolar neurons are characterized by a large soma and long axon, while Golgi Type II multipolar neurons are smaller. This thesis focuses primar-

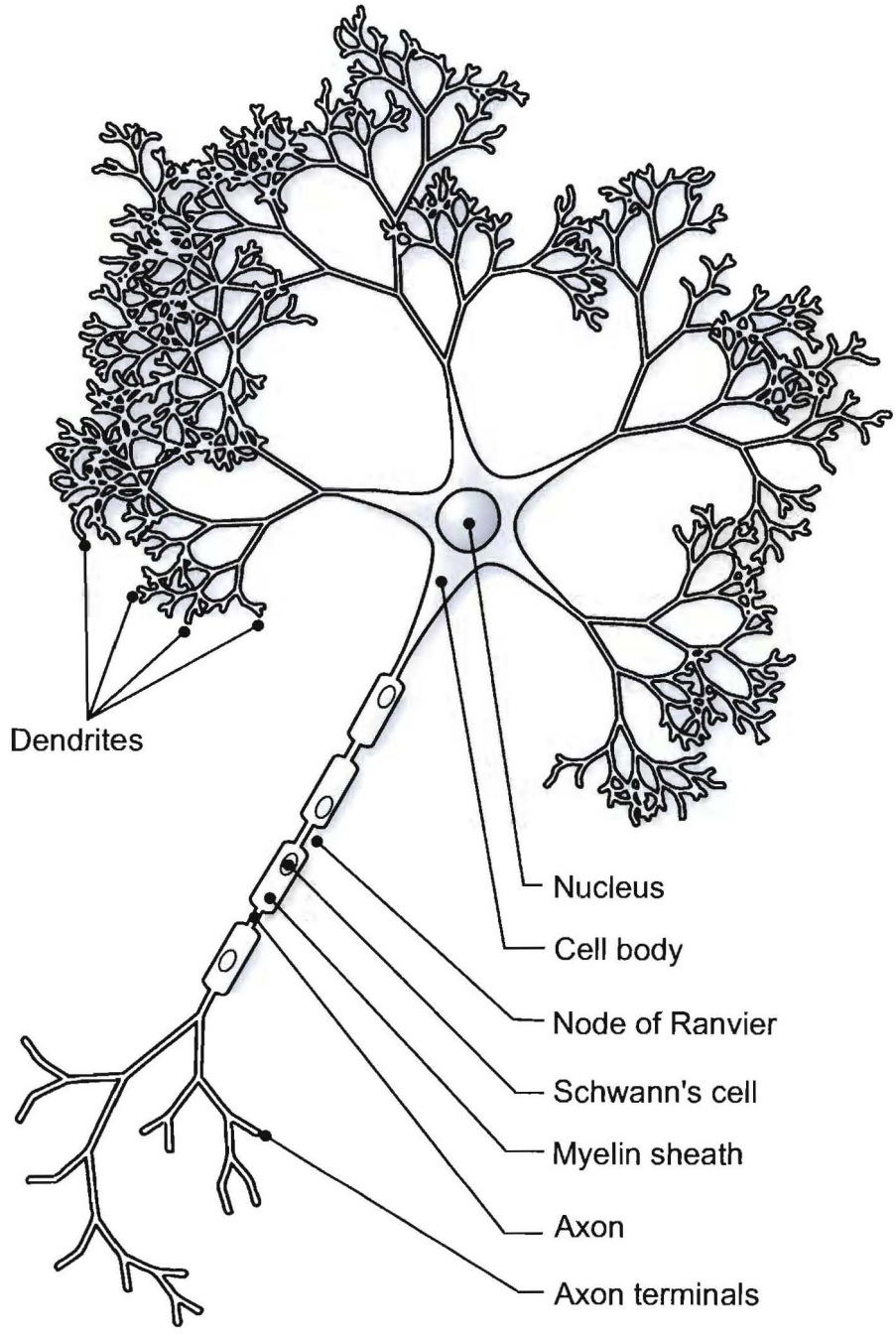

Figure 3.1: A diagram of typical neuron. From http://commons.wikimedia.org/wiki/File:Neuron-figure.svg. Used under the GNU Free Documentation License.

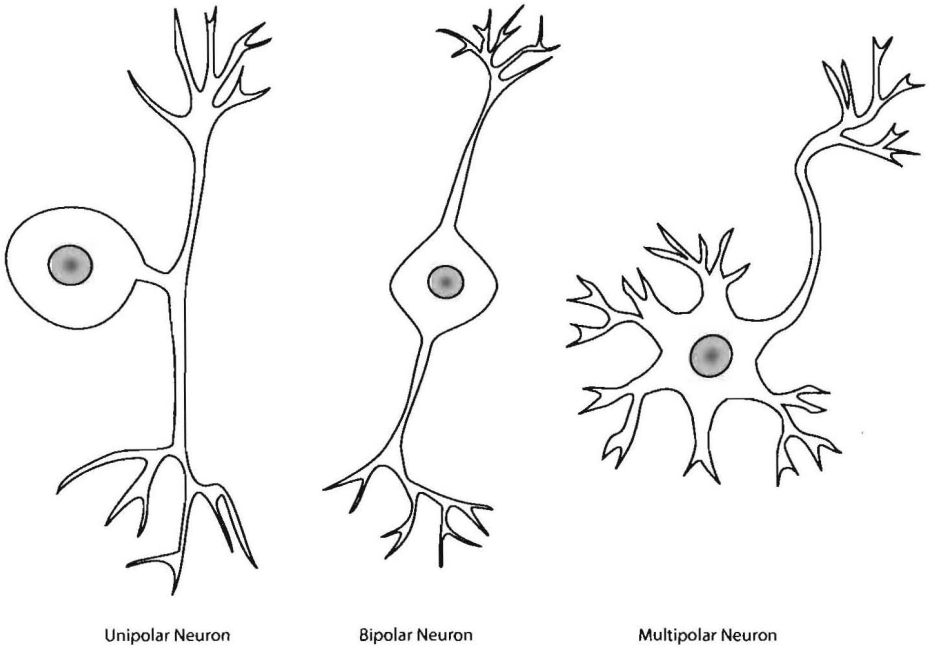

Figure 3.2: A diagram showing a unipolar, bipolar, and multipolar neuron. Adapted from http://commons.wikimedia.org/wiki/File:Neurons_uni_bi_multi_pseudouni.svg. Used under the Creative Commons Attribution-Share Alike 3.0 Unported License

ily upon tissue within the cerebral cortex (see below for a discussion of the parts of the brain), where so-called pyramidal cells play a major role. Pyramidal cells are prime example of Golgi Type I multipolar neurons [40].

In axons, the transmission of neural signals occurs primarily electrically through so-called action potentials. Action potentials are a self-propagating inflow and outflow of ions (primarily sodium and potassium, respectively, though chloride plays a role too) that travel down the length of an axon. Action potentials are made possible by the fact that axons contain certain ion gates and ion pumps that allow them to maintain a slight imbalance between positive and negative charges across their membrane, resulting in a potential difference of roughly 70 mV when resting. When an external stimulus of sufficient magnitude is applied to the neuron, the energy stored in this potential difference suddenly discharges to produce an action potential that travels down the axon, with a duration of roughly 5 ms [28, 40]. Although the precise details are rather complicated, Hodkin and Huxley's Nobel-prize-winning differential equation model describes the chief features of the process relatively well. In this model, the all-or-nothing characteristic of action potentials is explained as a consequence of the nonlinear relationship between the currents and voltages across the membranes of axons [13].

In contrast to axons, dendrites send and receive messages in a primarily chemical fashion through the use of neurotransmitters (biomolecules) like GABA and glutamate [3, 12]. The transmission of information between neurons occurs at synapses, which form the connections between axons and dendrites. Although both electrical and chemical synapses exist within the human body, the majority of them are chemical [28]. This thesis presents a mathematical model that tries to understand certain aspects of dendrite communication.

Although neurons are the basic cellular units of the nervous system, major differences still exist between the different parts of the nervous system. For example, the human brain is composed of five main parts: the brain stem, the thalamus, the hypothalamus, the cerebellum, and the cerebrum. Functionally, each part of the brain is responsible for a different task. For example, the brain stem and the hypothalamus are responsible for breathing and appetite regulation, respectively. In terms of cognition, the cerebrum is the most important part of the brain [28]. Because of the cerebrum's importance for this thesis, we discuss its features in somewhat closer detail.

In humans and in most mammals, the cerebrum is the most conspicuous feature of the brain, and it is divided structurally into several parts. First of all, the cerebrum is divided into left and right cerebral hemispheres. Secondly, the cerebrum can be thought of as divided into white matter and gray matter. White matter is found deep in the cerebrum and is composed primarily of myelinated (sheathed) axons that form connections to other portions of the brain [28]. The grey matter - or cerebral cortex - is what most people likely visualize when they hear the word brain. The cerebral cortex is a relatively large ($\sim 60\,cm^2$), sheet-like mantle approximately $1.5 - 4.5\,mm$ in thickness. Because of its large size relative to the skull, the cerebral cortex folds to form sulci (grooves) and gyri (peaks) [40]. This distinctive morphology allows the cerebral

cortex to maximize surface area while minimizing volume. This is a key feature for humans, since a correlation exists between the number of folds and the complexity of brain functioning possible. Finally, in humans and mammals the bulk of the cerebral cortex is known as the neocortex (neo- for new, in the evolutionary sense) because of its characteristic internal structure [28]. The neocortex has a laminar structure and is divided into six different strata, each with slightly different functional and structural attributes. Although a detailed description of the differences between these layers is interesting in its own right, it suffices to say that many dendrites are found in the molecular lamina and the external granular lamina, the most superficial (i.e., the shallowest) two layers of the neocortex [40]. In the discussion that follows, the dendrites are assumed to be in these general regions of the human brain.

Chapter 4

Overview of Classical Physics

It is well-known that all matter possesses the property known as mass, which serves both as a measure of the quantity of a substance and of the gravitational attraction of the substance to other massive bodies. Classically, gravity is described by Newton's famous universal law, which says that the gravitational force between two objects is directly proportional to the product of their masses and inversely proportional to the square of their separation [43]:

$$F_{grav} = k_{Newton}\frac{m_1 m_2}{r^2} \tag{4.1}$$

Perhaps somewhat surprisingly, many mathematical and physical parallels - but also important differences - exist between familiar gravitational phenomena and electrical and magnetic phenomena. For this reason, analogy and comparison can provide an instructive introduction to electricity and magnetism.

First of all, all matter possesses a certain intrinsic electrical quantity known as charge. Unlike mass, which must be strictly greater than zero, electrical charge may be positive, negative, or zero. This variety means that electrical forces may attract, repulse, or even fail to exist between two objects, a stark contrast to the ever-present, ever-attractive gravitational force. Secondly, the electrical force between two charged objects is described by Coulomb's law, which miraculously possesses precisely the same mathematical form as Newton's law of gravitation [43]:

$$F_{elec} = k_{Coulomb}\frac{q_1 q_2}{r^2} \tag{4.2}$$

Evidently, the only difference between the laws is the substitution of charge q for mass m and of Coulomb's constant $k_{Coulomb}$ for Newton's constant k_{Newton}.

Another important difference reveals itself when one considers the effects of moving bodies. In classical physics, the gravitational force between two massive bodies is the same regardless of whether not they are moving. The corresponding statement is emphatically not true for moving electrically charged bodies.

Indeed, Coulomb's law does not tell the whole story, since two objects in any sort of relative motion also exert magnetic forces on each other according the so-called Biot-Savart law (which I present in Chapter 7). Equivalently, one may say that the fundamental cause of all magnetic phenomena is moving electrical charge, i.e., electrical current. In the case of everyday bar or refrigerator magnets, the relevant motion comes from the bound electrons of the atoms in the magnet. Although a full explanation requires the application of the techniques of modern physics and quantum mechanics (the Bohr-van Leeuwen Theorem states the result precisely [22]), the general idea is entirely straightforward.

Another critical concept in physics is that of a field. Physicists often speak of gravitational, electric, or magnetic fields, and their meaning is intimately tied to the force laws given above in Eqs. (4.1) and (4.2). Clearly, the force between two objects depends on their separation as well as their mass or charge, respectively. As it turns out, a useful way to think about this is to consider some massive (or charged) object and the force it would exert upon some hypothetical massive (or charged) object placed at some distance away from it. In other words, instead of thinking about the force between two objects, one focuses instead on the capability of one object to exert forces on others, independent of whether or not they are actually there. This capability to exert a force is roughly what physicists mean when they say field [8]. Using this new language, one may say that mass, charge, and current are the sources for gravitational, electric, and magnetic fields, respectively. In Figure 4.1 below, one can see the electric field lines between positive and negative electrical point charges. A hypothetical positive test charge placed in the vicinity of the charges would experience an electrical force in the direction given by the arrows, with the higher line densities close to the charges corresponding to larger forces.

The reader may have also noticed that no distinction has yet been drawn as to the precise form of an electrical current the produces magnetic forces and fields. Indeed, a host of technical applications - ranging from modern computers to locks in car doors - is made possible precisely by the fact that any current whatsoever produces magnetic effects. This characteristic is especially important in medical studies, where magnetic resonance imaging (MRI) and magnetoencephalography (MEG) provide a window into the human body by measuring the magnetic fields generated by flows of ions (charged particles) dissolved in blood and other bodily fluids. Although more details will be forthcoming, the idea that the chemical currents from dendrite activity produce magnetic effects is one of the central ideas of this thesis.

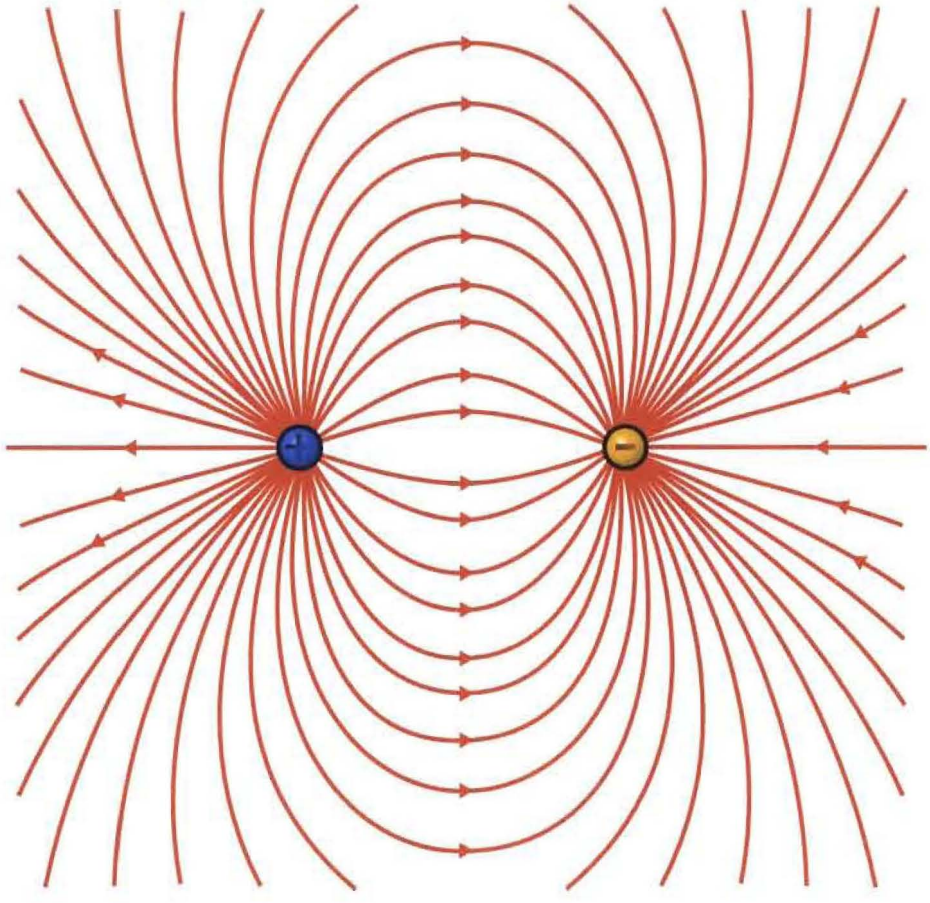

Figure 4.1: A diagram showing the electric field lines between positive and negative point charges. From http://commons.wikimedia.org/wiki/File:VFPt_dipole_electric_manylines.svg. Used under the GNU Free Documentation License.

Chapter 5

Introduction to Magnetic Resonance Imaging

As the title of the thesis suggests, an elementary understanding of magnetic resonance imaging (MRI) is necessary for an appreciation of what follows. Following the approach of Chapter 4, we proceed by appealing to analogies.

Anyone who has ever played with a toy top is already familiar with a close analog to the general principle responsible for MRI. As experience tells us, a top will remain in a vertical position as long as it is spinning. Closer inspection, however, reveals that the top does not maintain a perfectly vertical orientation; instead its axis of rotation moves gradually about the vertical axis. This behavior is well understood and is known to physicists as precession. What's more, precessional behavior is exhibited by most spinning objects subject to a uniform (or essentially uniform) external field. In the case of the toy top, the relevant field is the earth's gravitational field, which is nearly uniform near the earth's surface. Another familiar example of precession is found with the earth itself, which precesses as it spins in its orbit around the sun [43]. Figure 5.1 below is a diagram showing the precession of a spinning top in a gravitational field.

Modern physics has shown that spin is not reserved for macroscopic objects. Indeed, the familiar subatomic particles of electrons, neutrons, and protons all possess a spin property which is sensitive to magnetic fields instead of gravitational fields. In this case, the subatomic spins can be made to precess when placed in an external magnetic field [43].

The second important physical property exploited by MRI is resonance. Resonance is a widely observed phenomenon through which oscillating systems absorb energy. Again, a conceptually familiar example may be found in a gravitational system, this time in the form of a standard playground swing set [14]. As childhood experience reveals, in order to increase the height (i.e., energy) of one's flight while swinging, one must move his or her legs back and forth with a certain steady frequency; faster or slower leg movement is somehow less effective. This specific frequency is known as the resonant frequency of the

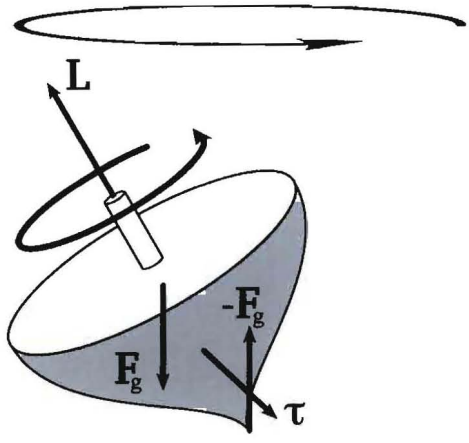

Figure 5.1: A diagram showing the precession of a spinning top. From http://commons.wikimedia.org/wiki/File:PrecessionOfATop.svg. Used under the Creative Commons Attribution-Share Alike 2.5 Generic License.

system. In the case of precessing protons, a closely related resonance behavior occurs in the presence of an oscillating magnetic field. What's more, a careful analysis of proton behavior shows that this microscopic resonance behavior is very sharply peaked about its resonant frequency. In other words, a precessing proton only absorbs energy when exposed to oscillating magnetic fields within a precise frequency band; applied frequencies from outside this band will not excite (i.e., add energy to) the spin system.

Since the human body is composed primarily of water (H_2O), the body contains an abundance of hydrogen atoms, whose nuclei consist of single protons. Hence the previous discussion of the behavior of protons in magnetic fields may easily be applied to the human body by virtue of the abundance of water therein. When a MRI machine applies a large, uniform magnetic field, $\vec{B}_0$, to the patient, the protons will tend to align themselves into one of two energy states characterized by parallel or antiparallel orientation of the spins with respect to the magnetic field. In other words, the spins tend to line up either in the direction of the magnetic field or directly opposed to it. In a typical MRI system, the applied magnetic field is on the order of teslas (the SI unit of magnetic field strength). For comparison, these magnetic fields are approximately 10,000 times stronger than the magnetic field of the earth [34].

Because the protons in the body possess spin, they will begin precessing around the direction of the applied magnetic field at a specific frequency, $\omega = \gamma \cdot B_0$, known as the Larmor frequency. Here γ is a physical constant known as the gyromagnetic ratio of the proton, and its value is known from quantum mechanics. Through the application of a brief oscillating magnetic field (a radio-frequency, or RF, pulse), the precessing spin states can be made to absorb energy. However, just as the amplitude of the oscillations of a swing decreases

when the kicking stops, the atomic spin states will also fall back into their original spin state after the end of the RF pulse. During this transition, or relaxation, the spins produce a time-changing magnetic field (since the transition corresponds to a change in the total magnetization of the tissue), which produces measurable electrical effects via Faraday's Law. This is the same law harnessed by electric generators that use water, wind, or even internal combustion to spin magnets and produce electrical currents. Finally, the computer equipment in the MRI system records and analyzes the electrical effects of this spin relaxation.

By applying a slightly non-uniform, or gradient, magnetic field to the human body, one can cause the protons in different parts of the body to precess with slightly different Larmor frequencies. In this way, one can selectively choose which areas of the body absorb energy when the RF pulse is applied. Since spin relaxation times depend on local tissue properties (i.e., different tissues respond differently to RF pulses), the structural differences within the body become evident in the electrical signal recorded by the MRI computers. Using this data, the machine is able to construct the familiar MRI images like those found in standard anatomy textbooks. An example of an image produced by an MRI scan can be seen below in Figure 5.2.

MRI has been used all over the body and has proven to be an especially invaluable tool for researchers wishing to study the brain noninvasively. Moreover, the physical principles discussed above also carry the ability to image indirect indicators of brain activity through a phenomenon known as blood-oxygenation-level dependent (BOLD) contrast. The imaging process that uses BOLD contrast is known as functional magnetic resonance imaging (fMRI) or BOLD fMRI. BOLD contrast refers to the observation that the signal generated by the relaxing magnetization after an RF pulse depends on level of deoxygenated hemoglobin in the red blood cells of the tissue being imaged. This contrast arises because hemoglobin molecules have different magnetic properties based on whether or not they have a bound oxygen molecule [14]. Briefly stated, fMRI looks for the spin relaxation of protons in blood in regions where the surrounding tissues were not excited (i.e., were off resonance). The implication then is that the blood was sent to these tissues as a response to neural activity. Thus, fMRI provides an indirect method for measuring and mapping neural activity [14].

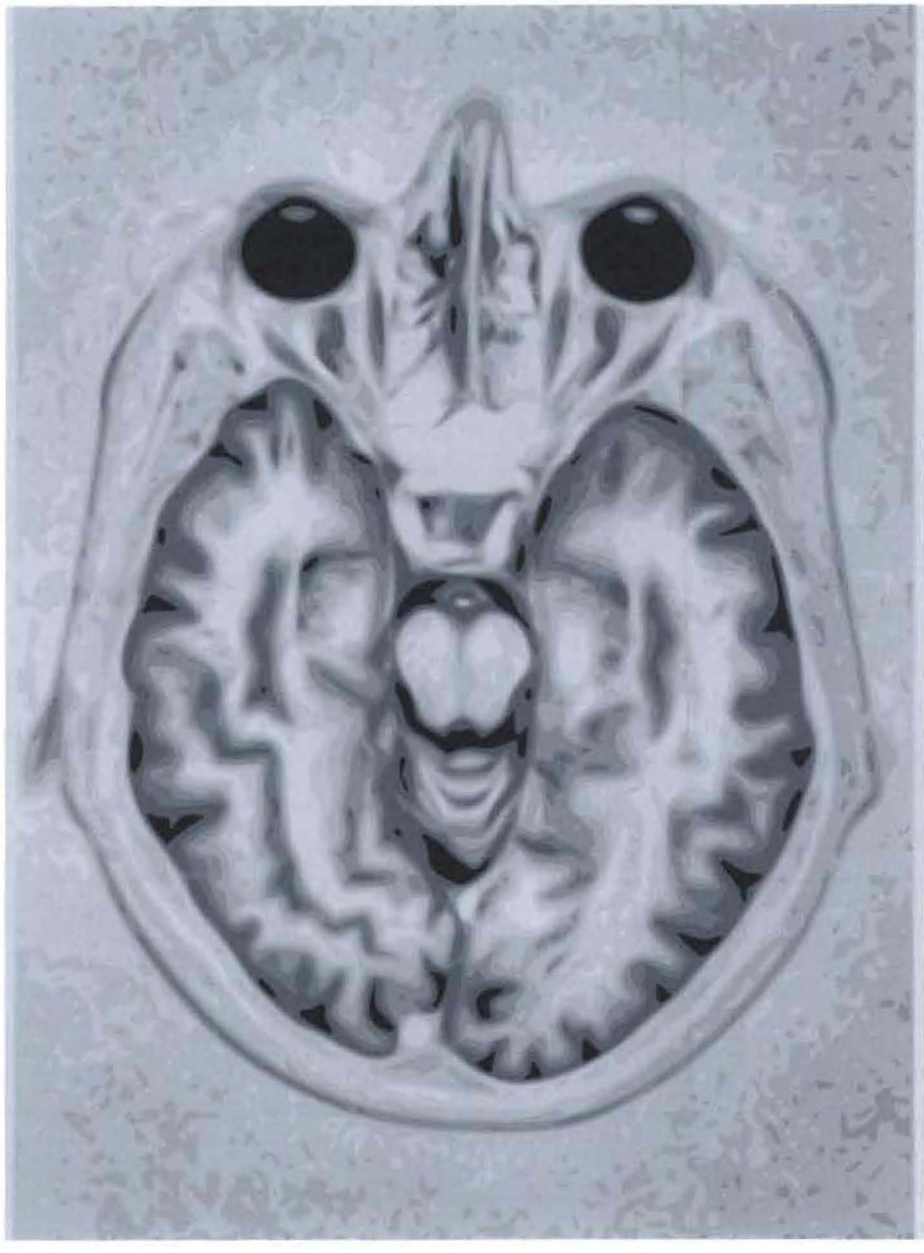

Figure 5.2: An example of an image produced using MRI. © Nevit Dilman. From Wikimedia commons: http://commons.wikimedia.org/wiki/File:Brain_Mri_nevit.svg. Used under the Creative Commons Attribution Share Alike 3.0 Unported License.

Chapter 6

Direct Detection of Neural Activity

Chapter 5 described how fMRI gives scientists a non-invasive probe for studying the brain. However, imaging based on BOLD contrast is fundamentally limited in a couple of important respects, all stemming from the fact that the measured signal is an indirect marker of activity. First, because BOLD looks for perfusion (blood flow to active tissues), there is a time delay between when the tissues are neurologically active and when the body responds by sending energy in the form of blood to the neurons. Secondly, when blood flows to active tissues, it does so from all directions. Although neural activity may exhibit tight spatial localization, the detail can become blurred by the perfusion process. In essence, the best possible resolution using BOLD techniques is fundamentally limited in nature [14]. A potential solution to these limitations is direct measurement of neural activity.

Chapter 3 described how the nervous system transmits information using electrical and chemical signals, which correspond physically to small fluid currents. Because neural fluids contain a wealth of ions such as K^+, Na^+, and Cl^-, these currents will also generate associated magnetic fields according to general principles given in Chapter 4. From the point of view of the protons in the body, this biomagnetic field is on equal footing with the substantially larger applied field of the MRI machinery. Thus, the observed Larmor frequency of the precessing protons in regions of neural activity should differ slightly from the predicted frequency based on the applied field. By looking for these discrepancies in the measured signal, one should be able to work backwards and identify regions of activity. In this fashion, one could theoretically exploit the full resolution of MRI without the limitations of fMRI based on BOLD techniques. Armed with direction detection of neural currents, scientists could address a number of outstanding questions. For example, doctors interested in degenerative diseases of the brain might gain a better understand of disorders like Alzheimer's disease, Parkinson's disease, or multiple sclerosis. Neurosurgeons would gain a

new method for measuring nerve conduction velocities noninvasively, and cognitive scientists could directly map active regions of the brain. Clearly, direct detection would be an immediate boon to many fields of scientific inquiry.

The idea of direct imaging is by no means new. Although many researchers have tried to measure neural currents using MRI [4, 5, 11, 16, 17, 24, 31], the true feasibility of direct detection remains controversial [1, 19, 42]. In the past researchers have sought to calculate the magnetic fields associated with action potentials [5,24], and numerical studies have found the magnetic fields of nerves, muscles, and even single axons [30, 33, 41]. Experimentally, considerable work has been done using ferrite-core, wire-wound toroids [9, 10, 27, 32, 33, 35, 37–39], and numerous other experimental models to simulate and study the problem [2, 4, 5, 20]. As mentioned above, the results of these studies have been mixed, with some claiming measurable effects [4, 25, 42] and others reporting that the currents and fields of the brain are simply too weak to generate significant effects in MRI signals. The goal of the research of this thesis has been to investigate a specific kind of neural activity - that of dendrites - in an effort to help clarify the question of direct detection.

As the situation now stands, it is natural to ask why dendrites have been singled out. The answer to this question is twofold. First of all, the magnetic fields of axons have already been studied in some detail, and the salient features are reasonably well-understood [27, 35, 37, 39, 41]. More importantly, although the action potentials of axons are expected to generate larger magnetic fields than dendrites, they also move with significantly faster velocities. For comparison, action potentials travel at roughly 1 to 10 m/s in unmyelinated axons and up to an order of magnitude faster for myelinated axons [28], while dendritic currents travel at speeds of roughly 0.05 to 0.08 m/s [26]. Because of the time necessary for a typical MRI imaging sequence (RF pulses, relaxation, and measurement), the faster speeds of axons make them more difficult to detect. Thus, dendrites have been chosen as a more promising candidate for detection in spite of their comparatively small magnetic fields.

Chapter 7

A Mathematical Model of Dendritic Magnetic Fields

7.1 General Remarks

Just as electric fields from an arbitrary charge distribution may calculated from Coulomb's Law, the magnetic field produced by a distribution can be calculated using the well-known Biot-Savart Law [15]:

$$\vec{B} = \frac{\mu}{4\pi} \int \frac{I\, d\vec{l} \times \hat{r}}{r^2} \tag{7.1}$$

where I is the current, r is the spatial position, μ is the magnetic permeability, and $d\vec{l}$ is a differential length element. Although the presence of the integral makes the Biot-Savart Law mildly more formidable, it bears formal resemblances to Newton's Law and Coulomb's Laws. For example, the $1/r^2$ dependence and the direct proportionality to the field sources is common to all three laws (here current takes the place of mass or charge). In order to model a physical system with the Biot-Savart Law, one must select a current distribution to generate the field. In the study of biomagnetic fields (and also a larger class of problems) a common approach is to model the various magnetic field sources as current dipoles [18, 19]. Roughly speaking, current dipoles behave like small bar magnets. The justification for this method stems from the fact that the magnetic field from an arbitrary current distribution may be written in the form of a so-called multipole expansion [15]. In this form, the expression for the magnetic field is written as an infinite series (i.e., a sum) in which each term describes the magnetic field associated with a symmetry of the distribution. The main contribution to this expression generally comes from the leading dipole term, and the rest of the infinite series may be neglected. Only in the case of intricate symmetries do higher-order terms play a major role, and these special symmetries are not expected to be present in the brain. Thus, at least as a first approximation, one expects the magnetic fields of the brain to be dipole in nature.

Roughly speaking, this approach seeks to identify and model the features of the brain's magnetic behavior which are most important. Previous studies [18, 19] have modelled large portions of the brain using tens to hundreds of dipoles, and the research of this thesis expands this idea by modelling individual dendrites as dipoles, an approach made feasible and attractive by advances in computing speed.

In the case of a dipole source, Eq. (7.1) (the Biot-Savart Law) may be integrated to yield the following expression:

$$\vec{B} = \frac{\mu}{4\pi} \frac{\vec{p} \times \vec{R}}{R^3} \tag{7.2}$$

where $\vec{p}$ is the current dipole, $\vec{R}$ is the vector from the dipole at some source point to the field point where the field is measured. In MRI, only one component of the magnetic field contributes to the precessional frequency described in Chapter 5. Without loss of generality, we choose a coordinate system in which the relevant component is parallel to the z-axis. Eq. (7.2) may then be evaluated to give the following expression for the z-component of the magnetic field from a current dipole:

$$B_z = \frac{\mu}{4\pi} \frac{p_x(y-y') - p_y(x-x')}{((x-x')^2 + (y-y')^2 + (z-z')^2)^{3/2}} \tag{7.3}$$

Here the primed coordinates refer to the source point, while the unprimed coordinates refer to the field points. Although the brain is a highly nonlinear system, the phenomenon of magnetism is always linear with regards to the combination of fields, and so the resultant field from multiple dipoles (i.e. dendrites) will simply be a linear superposition (sum) of fields given by Eq. (7.3) above.

7.2 Details of the Model

Because we are interested chiefly in an upper bound on the potential effects of dendritic activity on MRI signals, we make a number of simplifying assumptions in constructing the mathematical model.

1. All dendrites in a voxel (a $1\ mm^3$ volume-pixel) are arranged on a variable lattice structure
2. All dendrites are synchronously active
3. All dendrites have the same physical properties
4. The surrounding medium is homogenous and isotropic

Clearly, these assumptions provide a crude approximation of the complex geometries present in actual neural tissue. However, they make the problem computationally tractable, and the effects of these assumptions will be discussed thoroughly in what follows.

The mathematical model described above has several input parameters, namely, dendrite strength, spacing, and orientation. The empirical value for dendrite density in human cortical tissue is on the order of $10^6/mm^3$, and our simulations consider the effects of this density as well as several others [23]. In general, we treat only the case of uniform densities. Dendrites range greatly in length from around $300\,\mu m$ for an apical dendrite down to around $10\,\mu m$ for the shortest branching dendrites, and a given tissue volume will often have a larger number of the shorter dendrites [16]. As such, this model assumes all dendrites to have an average length of $L = 30\,\mu m$. Assuming that each active dendrite has an intracellular current of $I = 1\,nA$ [5,25], this gives an equivalent current dipole for a dendrite:

$$\vec{p} = \vec{I} \cdot l = 3 \times 10^{-5}\, nAm,$$

essentially a measure of the dendrite strength. As mentioned above, dipole orientation is also an input parameter in our model. Clearly, the maximum resultant magnetic field from some ensemble of dipoles will arise from parallel orientations. In other words, if the dipoles are not parallel, destructive interference will provide large-scale cancellation and reduction of the magnetic field. Although we explore the extent of this cancellation effect through simulations with randomly oriented dipoles, most simulations consider parallel orientations.

The final piece of the mathematical model is the calculation of the magnetic field's predicted effect on an MRI signal. As introduced in Chapters 5 and 6, the biomagnetic field generated by the active dendrites contributes to the phase of the precessing magnetic moments within a tissue, which is what MRI actually detects. To identify this effect, one looks at the difference between the measured phase and the predicted phase in the absence of the neural activity, a quantity known as the phase shift of the MRI signal. The phase shift due to the dendritic magnetic field at the field point (x, y, z) in an active volume of tissue be calculated according the following equation [42]:

$$\varphi(x, y, z) = \int_0^{TE} \gamma \cdot B_z(x, y, z, t)\, dt \tag{7.4}$$

In the above equation, TE is the so-called echo time of the MRI echo sequence, while γ is the gyromagnetic ratio of the proton, a known value from quantum mechanics of $2.7 \times 10^8\, s^{-1}T^{-1}$ [36]. In our calculations, we approximate this integral by assuming that the dendrites are active for a time less than echo sequence of the MRI, which allows the magnetic field B_z to be taken outside the integral. Thus, the phase shift is approximately the product $\varphi \approx \gamma \cdot B_z \cdot t_{act}$, where t_{act} is the activation time of the dendrites, taken to be approximately 0.01 seconds ($t_{act} << TE$). On purely physical level, the phase shift φ is essentially a measure of the change in angle between the precessing net magnetization before and after neural activation.

The experimenters Bodurka and Bandettini [4] measured the minimum detectable MRI phase shift in a model system using current-carrying wires in a saline bath. According to their results, a minimum phase shift of $0.1\,^\circ$ (0.0017

radians) is detectable. This thesis accepts their value as a working threshold for detection. However, for a number of reasons discussed later, their threshold seems optimistic, and the true minimum phase shift for detection is likely considerably larger.

Table 8.1: Summary of maximum simulated magnetic fields and phase shifts

	Dendrite Density (dipoles / mm^3)	Maximum B-Field (nT) (Threshold: 0.1 nT)	Phase Shift (radians x 10^{-3}) (Threshold: 1.7×10^{-3})
Line 100	100	0.005	0.013
Layer (10000)	10000	0.24	0.642
Full Voxel	$10^3 = 1000$	0.01	0.027
Full Voxel	$20^3 = 8000$	0.06	0.161
Full Voxel	$30^3 = 9000$	0.19	0.508
Full Voxel	$40^3 = 64000$	0.47	1.257
Full Voxel	$50^3 = 125000$	0.92	2.461
Full Voxel	$60^3 = 216000$	1.60	4.280
Full Voxel	$70^3 = 343000$	2.54	6.759
Full Voxel	$80^3 = 512000$	3.80	10.17
Full Voxel	$90^3 = 729000$	5.41	14.47
Full Voxel	$100^3 = 1000000$	7.43	19.88
Full Voxel	$215^3 = 9938375$	62.1	166.1
Full Voxel (Rand.)	10000	0.09	0.241
Full Voxel (Rand.)	50000	0.13	0.348
Full Voxel (Rand.)	100000	0.41	1.097
Full Voxel (Rand.)	$50^3 = 125000$	0.056	0.150
Full Voxel (Rand.)	1000000	0.22	0.589

Chapter 9

Analysis and Discussion

9.1 Implications

The goal of this study was to generate a theoretical model that could describe the magnetic fields generated by the receptor potentials of dendrites in grey matter in human cortical tissue and to assess the possibility of detecting the responsible currents using MRI. Taken as a whole, the results show that under the most ideal circumstances dendritic activity might barely be detectable using present MRI technology. Recalling from above that 10^6 dendrites per mm^3 is the realistic value for the human body, one sees from Table 8.1 and Figure 8.3 that 10^6 simultaneously active, uniformly oriented dendrites could generate a magnetic field and associated phase shift above the threshold given by Bodurka and Bandettini [4]. This situation is unlikely to occur within the human brain under normal circumstances, although some evidence suggests that such activity might occur during an epileptic seizure [29]. More realistically, dendrites may be expected to orient themselves randomly, and simulations with random dendrite orientation (see Table 8.1) show phase shifts well below the detection threshold. However, it is also reasonable to believe that the dendrite orientations are not perfectly random, but instead exhibit some uniform behavior on small distance scales and more random behavior on distance scales on the order of the size of the voxel considered in the simulations. In Figure 8.4 one can see the z-component of the magnetic field generated by a random distribution of dendrite orientations. One of the salient features of this plot is the large number of closely-spaced local maxima and minima. If there were small-scale correlations in the dendrite orientations, one would expect the local maxima and minima to spread apart, which would have a bearing on the phase shift produced in the MRI signal. Although correlation effects are an interesting phenomenon, they would simply provide a refinement on the upper and lower bounds for the phase shift given by the uniform and random orientations, respectively. If direct detection becomes a reality in the future, simulations of the effects of correlation lengths may become important. At present, such a study would provide more

detail than necessary.

As mentioned previously, the results of the simulations likely overestimate the effects of dendrites on an MRI signal for a variety of reasons:

1. The biphasic signal (see Chapter 8) of dendrites is very difficult to capture in real-world applications. The reason for this is that the symmetry produced by the rising and falling fields (which arises from the depolarization and repolarization of the transmembrane potential of the dendrite) will integrate nearly to zero in Eq. (7.4). The intuitive reason for this is that time-average of the biomagnetic field is approximately zero, since an entire dendrite signal lasts only a few milliseconds. One way around this difficulty would be the development of quick, carefully-timed pulse sequences that could detect the depolarization phase (the rise in the field) before the repolarization (the fall in the field) counteracts the phase shift.

2. The signal recorded in MRI also represents a spatial-average of the magnetic field in an active voxel. In calculating the phase shifts given in Table 8.1 by approximating Eq. (7.4), this effect was not considered. Because the relatively tight spatial localization of the extrema in Figures 8.1, 8.2, and 8.3 one sees that the spatial average will likely produce a much smaller signal.

3. The dendrites in a voxel will generally not be simultaneously active. Instead, some dendrites will be repolarizing while others are depolarizing, and others still may simply be inactive. The simulations involving fewer than 10^6 dendrites account at least partially for this effect, since they may be interpreted as the case in which there is an excess of dipoles in the depolarization or repolarization state and in which the other states completely cancel. Clearly this is an idealization, but the general decrease in phase shift shown in Table 8.1 should remain unchanged.

4. All simulations have assumed that the dipoles are fixed in horizontal planes. In the brain dendrites may of course have components in the z-direction. Because of the mathematical form of the vector cross product $\vec{p} \times \vec{R}$ in Eq. (7.2) above, these components will contribute neither to the z-component of the magnetic field nor the detected phase shift.

Another important consideration is the validity of the threshold values proposed by Bodurka and Bandettini [4]. In their experiment, the threshold phase shift of $0.1°$ was established using a voxel some 20 times larger than the voxels in the present simulations. Furthermore, their experiment considered magnetic fields produced by wires, which (to first-order approximation) decrease like $1/r$ with distance, while the fields from dipoles decrease more quickly with distance, as Eq. (7.2) above shows. In general, a larger field averaged over a large voxel should correspond to a reasonably large signal. In this sense, the experimental model used is not a realistic model of living tissue. When the difficult-to-quantify effects of physiological noise (which Bodurka and Bandettini do address) are also considered, one leaves with the impression that although

$0.1°$ may be an accurate detection threshold for some applications, the minimum detectible phase shift in the brain should likely be higher. Thus, although Bodurka and Bandettini's threshold provides a useful and instructive starting point for analysis, it seems optimistic and should be viewed with appropriate care concerning its domain of applicability.

In conclusion, my simulations show that the neural currents of dendrites may barely be detectable using current technology in extreme cases like seizures, but direct detection of normal brain activity remains unlikely. Nevertheless, MRI researchers continue to develop clever new imaging methods, either using sophisticated pulse sequences or data processing, and perhaps future technology will provide new solutions.

9.2 Moving Forward: A Look to the Future

In a glance toward the future, one promising technology in the search for direct detection of neural activity is ultra-low field MRI. Ultra-low field MRI functions on many of the same principles as traditional MRI, but uses a dramatically smaller applied magnetic field (on the order of $1 - 100\,\mu T$) to align the precessing spins. In general, the idea is that the phase shift from biomagnetic field is essentially independent of the applied magnetic field. By lowering the applied field, the fractional change on the measured signal due to neural activity would be increased. Another key difference in ultra-low field MRI is the use of superconducting quantum interference devices (SQUIDs) to sample the magnetic fields present in tissue just prior to depolarization, an approach known in the literature as "multimodal." The development of techniques like these has been pioneered in part by R. McDermott and his collaborators at the University of California, Berkley [21]. Although ultra-low field MRI has a variety of potential applications, including testing for liquid explosives at security checkpoints [7], the prospect of direct detection of neural activity is certainly one of the most exciting and one that has not escaped the notice of MRI community. To my knowledge, this possibility was first mentioned in the literature by Kraus et al. in 2008 [20]. In this paper, the authors used current phantoms (a type of experimental model) to test the detectability of neural activity using the aforementioned multimodal methods. In response to this paper, Cassara and collaborators conducted a focused computational investigation [6] of similar flavor (but significantly more intricate) to the one presented in this thesis and highlighted some of the technical questions that the scientific community must address in order for ultra-low field MRI to live up to its considerable promise. Clearly, we are in an exciting time as scientists continue to search for better windows into the human mind, and I hope that my research has played at least some small role in the opening of these windows.

Bibliography

[1] P.A. Bandettini, N. Petridou, and J. Bodurka. Direct detection of neuronal activity with MRI: fantasy, possibility, or reality? *Appl. Mag. Reson.*, 26:65–88, 2005.

[2] P.A. Bandettini, E.C. Wong, R.S. Hinks, R.S. Tikofsky, and J.S. Hyde. Time course EPI of human brain function during task activation. *Magn. Reson. Med.*, 25:390–397, 1992.

[3] M.F. Bear, B.W. Connors, and M.A. Paradiso. *Neuroscience: Exploring the Brain.* Williams and Wilkins, 1996.

[4] J. Bodurka and P.A. Bandettini. Toward direct mapping of neuronal activity: MRI detection of ultraweak, transient magnetic field changes. *Magn. Reson. Med.*, 47:1052–1058, 2002.

[5] A.M. Cassara, G.E. Hagberg, M. Bianciardi, M. Migliore, and B. Maraviglia. Realistic simulations of neuronal activity: A contribution to the debate on direct detection of neuronal currents by MRI. *NeuroImage*, 39:87–106, 2008.

[6] A.M. Cassara and B. Maraviglia. Microscopic investigation of the resonant mechanism for the implementation of nc-MRI at ultra-low field MRI. *NeuroImage*, 41:1228–1241, 2008.

[7] M. Espy. Ultra-low-field MRI for the detection of liquid explosives. *Supercond. Sci. Technol.*, 23(3):4023, 2010.

[8] R. Feynman. *The Feynman Lectures on Physics, Vol. I.* Pearson Addison Wesley, San Francisco, 2006.

[9] F.L.H. Gielen, R.N. Friedman, and J.P. Wikswo. In vivo magnetic and electric recordings from nerve bundles and single motor units in mammalian skeletal muscle. *J. Gen. Physiol.*, 98:1043–1061, 1991.

[10] F.L.H. Gielen, B.J. Roth, and J.P. Wikswo. Capabilities of a toroid-amplifier system for magnetic measurement of current in biological tissue. *IEEE Trans. Biomed. Eng.*, 33:910–921, 1986.

[11] G.E. Hagberg, M. Bianciardi, and B. Maraviglia. Challenges for detection of neuronal currents by MRI. *Magn. Reson. Med.*, 24:483–493, 2006.

[12] C. Hammond. *Cellular and Molecular Neurophysiology.* Elsevier Academic Press, 2008.

[13] R.K. Hobbie and B.J. Roth. *Intermediate Physics for Medicine and Biology.* Springer, New York, 2007.

[14] S.A. Huettel, A.W. Song, and G. McCarthy. *Functional Magnetic Resonance.* Sinauer Associates, Sunderland, MA, 2009.

[15] J.D. Jackson. *Classical Electrodynamics.* Wiley, New York, 1999.

[16] D. Johnston, J.C. Magee, C.M. Colbert, and B.R. Christie. Active properties of neuronal dendrites. *Annu. Rev. Neurosci.*, 19:165–186, 1996.

[17] H. Kamei, K. Iramina, K. Yoshikawa, and S. Ueno. Neuronal current distribution imaging using magnetic resonance. *IEEE Trans. Magn.*, 35:4109–4111, 1999.

[18] L. Kaufman, J.H. Kaufman, and J.Z. Wang. On cortical folds and neuromagnetic fields. *Electroencep. Clin. Neurophy.*, 79:211–229, 1991.

[19] D. Konn, P. Gowland, and R. Bowtell. MRI detection of weak magnetic fields due to an extended current dipole in a conduction sphere: A model for direct detection of neuronal currents in the brain. *Magn. Reson. Med.*, 50:40–49, 2003.

[20] R.H. Kraus, P. Volegov, A. Matlachov, and M. Espy. Toward direct neural current imaging by resonant mechanisms at ultra-low field. *NeuroImage*, 39:310–317, 2008.

[21] R. McDermott et al. Liquid-state NMR and scalar couplings in microtesla magnetic fields. *Science*, 295(5563):2247–2249, 2002.

[22] W. Nolting. *Grundkurs Theoretische Physik 6: Statistische Physik.* Springer, Berlin, 2007.

[23] P.L. Nunez and R. Srinivasan. *Electric Fields of the Brain: The Neurophysics of EEG.* Oxford U.P., New York, 2006.

[24] M.N.J. Paley, L.S. Chow, E.W. Whitby, and G.G. Cook. Modeling of axonal fields in the optic nerve for direct MR detection studies. *Imag. Vision Comput.*, 27:331–341, 2009.

[25] T.S. Park and S.Y. Lee. Effects of neuronal magnetic field on MRI: Numerical analysis with axon and dendrite models. *NeuroImage*, 35:531–538, 2007.

[26] R.R. Pozanski. Conduction velocity of dendritic potentials in a cultured hippocampal neuron model. *Neurosci. Res. Comm.*, 28(3):141–150, 2001.

[27] B.J. Roth and J.P. Wikswo. The magnetic field of a single nerve axon: A comparison of theory and experiment. *Biophys. J.*, 48:93–109, 1985.

[28] E.P. Solomon, L.R. Berg, and D.W. Martin. *Biology.* Brooks and Cole, Belmont, CA, 2005.

[29] P. Sundaram, W.M. Wells, R.V. Mulkern, E.J. Bubrick, E.B. Bromfield, M. Munch, and D.B. Orbach. Fast human brain magnetic resonance responses associated with epileptiform spikes. *Magn. Reson. Med.*, 64:1728–1738, 2010.

[30] K.R. Swinney and J.P. Wikswo. A calculation of the magnetic field of a nerve action potential. *Biophys. J.*, 32:719–732, 1980.

[31] T.K. Truong and A.W. Song. Finding neuroelectric activity under magnetic field oscillations (NAMO) with magnetic resonance imaging in vivo. *Proc. Natl. Acad. Sci. USA*, 103:12598–12601, 2006.

[32] J.M. van Egeraat, R.N. Friedman, and J.P. Wikswo. Magnetic field of a single muscle fiber: First measurement and a core conductor model. *Biophys. J.*, 57:663–667, 1990.

[33] J.M. van Egeraat and J.P. Wikswo. A model for axonal propagation incorporating both radial and axial ionic transport. *Biophys. J.*, 64:1287–1298, 1993.

[34] A. Webb. *Introduction to Biomedical Imaging.* Wiley, Hoboken, New Jersey, 2003.

[35] R.S. Wijesinghe, F.L.H. Gielen, and J.P. Wikswo. A model for compound action potentials and currents in a nerve bundle III: A comparison of the conduction velocity distributions calculated from compound action currents and potentials. *Ann. Biomed. Eng.*, 18:97–121, 1991.

[36] R.S. Wijesinghe and B.J. Roth. Detection of peripheral nerve and skeletal muscle action currents using magnetic resonance imaging. *Ann. Biomed. Eng.*, 37(11):2402–2406, 2009.

[37] J.P. Wikswo, J.P. Barach, and J.A. Freeman. Magnetic field of a nerve impulse: First measurements. *Science*, 208:53–55, 1980.

[38] J.P. Wikswo, W.P. Henry, R.N. Friedman, W.A. Kilroy, R.S. Wijesinghe, J.M van Egegraat, and M.A. Milek. *Intraoperative recording of the magnetic field of a human nerve.* Plenum, New York, 1990.

[39] J.P. Wikswo and J.M. van Egeraat. Cellular magnetic fields: Fundamental and applied measurements on nerve axons, peripheral nerve bundles, and skeletal muscle. *J. Clin. Neurophsysiol.*, 8:170–188, 1991.

[40] J.L. Wilkinson. *Neuroanatomy for Medical Students.* Reed, Oxford, UK, 1998.

[41] J.K. Woosley, B.J. Roth, and J.P. Wikswo. The magnetic field of a single axon: A volume conductor model. *Math. Biosci.*, 76:1–36, 1985.

[42] X. Xue, X. Chen, T. Grabowski, and J. Xiong. Direct MRI mapping of neuronal activity evoked by electrical stimulation of the median nerve at the right wrist. *Magn. Reson. Med.*, 61:1073–1082, 2009.

[43] H.D. Young and R.A. Freedman. *University Physics with Modern Physics.* Pearson Addison Wesley, San Francisco, 2008.